Title

THE LOWEST TRIPLET STATE OF SUBSTITUTED BENZENES: II. THE PHOSPHORESCENCE MICROWAVE DOUBLE RESONANCE SPECTRA AND ORBITAL SYMMETRY OF THE 3nn* STATE IN PARADICHLOROBENZENE

Author

Buckley, M.J.

Publication Date

1971-11-01

LBL-409 c.2
Preprint

THE LOWEST TRIPLET STATE OF SUBSTITUTED BENZENES: II. THE PHOSPHORESCENCE MICROWAVE DOUBLE RESONANCE SPECTRA AND ORBITAL SYMMETRY OF THE $^3\pi\pi^*$ STATE IN PARADICHLOROBENZENE

M. J. Buckley, C. B. Harris, and R. M. Panos

November 1971

AEC Contract No. W-7405-eng-48

LBL-409 c.2

34

DISCLAIMER

THE LOWEST TRIPLET STATE OF SUBSTITUTED BENZENES: II. THE PHOSPHORESCENCE MICROWAVE DOUBLE RESONANCE SPECTRA AND ORBITAL SYMMETRY OF THE $^3\pi\pi^*$ STATE IN PARADICHLOROBENZENE

M. J. Buckley, C. B. Harris*† and R. M. Panos

ABSTRACT

Phosphorescence microwave double resonance (PMDR) spectra of para-dichlorobenzene have been obtained monitoring low temperature (~1.3°K) trap phosphorescence and used to make symmetry assignments of various vibronic bands present in the spectra. In addition, ratios of radiative rate constants of individual triplet spin sublevels to several vibrational bands, the intrinsic lifetimes of all three triplet spin sublevels, and selective polarized phosphorescence from individual spin sublevels to various vibrational bands have been measured. An analysis of these data is presented along with explicit considerations of the para-chlorine perturbation on the aromatic ring. Finally, the relationships between the orbital symmetries and the sign and magnitude of the zero-field electron spin dipolar interactions in the triplet state are presented for several halobenzenes and on these bases an assignment of the orbital symmetry of the lowest excited triplet state of p-dichlorobenzene is made.

---

* Alfred P. Sloan fellow

† To whom correspondence should be addressed.

Introduction

The classification of the orbital symmetry of excited triplet states of aromatic and substituted aromatic molecules is a problem which has received a considerable amount of attention from theoreticians and experimentalists alike. Early investigators, while attempting to establish the assignment of the lowest triplet state of benzene from a vibrational analysis of the phosphorescence, concluded that the transition was essentially dipole forbidden and that the weak phosphorescence activity originated from a vibronic coupling of the e_{2g} vibrations.[1] This vibronic coupling of the e_{2g} modes has been cited as evidence for either a $^3B_{1u}$ or $^3B_{2u}$ state.[1,2] Theorists have generally agreed that a $^3B_{1u}$ state would be lowest in energy.[3] In a classic study, Albrecht has set down the possible routes by which dipole allowed character might find its way into the benzene $T_1 \rightarrow S_0$ transition.[4] His findings, along with the oscillator strengths and phosphorescence polarization, allowed him to propose the $^3B_{1u}$ assignment which has since gained wide acceptance.

In addition to benzene, substituted benzenes such as hexachloro-, tetrachloro-, paradichloro- and paradibromobenzene have been studied. A $^3B_{2u}$ assignment has been proposed for the lowest triplet state of hexachlorobenzene on the basis of polarized phosphorescence spectra,[5] while single crystal polarized $T_1 \leftarrow S_0$ absorption spectra led Castro and Hochstrasser to propose an identical assignment for the p-dihalogenated benzenes.[6]

It is not generally possible, because of the spin-forbidden nature of phosphorescence transitions, to unambiguously assign the triplet orbital symmetry without a complete knowledge of the spin-orbit symmetries of all three triplet spin sublevels. Two techniques have been recently developed to determine these symmetries through an analysis of the spin sublevel origins in the vibrational bands of the phosphorescence spectrum.

The first, based upon the high-field Zeeman effect employed by Hochstrasser, et al.[7] has been effectively used to determine the magnitudes and signs of the zero-field parameters. Additionally, in cases where the applied magnetic field affects a resolvable splitting of the spin sublevels, this technique could be used to determine the symmetry of excited triplet states. The technique has the virtue of not restricting investigations to only the lowest triplet state since it can be applied to $T_1 \leftarrow S_o$ absorption spectra.

A second technique has evolved recently from the application of optically detected magnetic resonance[8] (ODMR) studies to molecules in phosphorescent triplet states. ODMR techniques have proven quite useful for the determination of a number of properties associated with excited triplet states, such as the zero-field splittings, nuclear-electron hyperfine and nuclear quadrupole interactions. Indeed, knowledge of these properties can shed light on the orbital nature of the triplet state. These techniques provide experimentalists with a powerful new tool, yielding data which, when incorporated into the wealth of spectroscopic data available, can remove the present ambiguities in the assignment of the orbital symmetries of excited triplet states in many molecules. For instance, it is well known that the magnitude of the zero-field parameter D is related to the spatial distribution of the electron spins[9] in the triplet state and can therefore be used to distinguish between an $n\pi^*$

and a $\pi\pi^*$ state. In addition to parameters directly related to the electron distribution in the triplet state, ODMR can be used to determine explicitly the intrinsic lifetimes of individual triplet spin sublevels and also their relative radiative activity to various vibrational bands present in the phosphorescence spectrum.[8,10] It is precisely these sort of data which are necessary for the unambiguous assignment of triplet state orbital symmetries. We have therefore applied ODMR techniques to the problem of determining the orbital symmetry of the lowest triplet state in paradichlorobenzene (DCB).

Experiment and Results

A. Sample

Samples of Eastman Organic paradichlorobenzene (DCB) were degassed and extensively zone-refined (200 passes at two inches/hour). Single crystals of DCB were grown by Bridgman techniques and mounted inside a helical slow wave structure which was suspended in a liquid helium dewar. When polarized data were collected crystals were aligned coniscopically to detect phosphorescence from the crystallographic bc face. The exciting light was incident on the a'b face and was incident from a direction perpendicular to the bc face. Temperatures lower than 4.2°K were obtained by pumping on the liquid helium.

B. Phosphorescence Microwave Double Resonance Spectroscopy (PMDR)

PMDR spectra were obtained in a manner similar to that previously reported.[11] Unpolarized phosphorescence emission was monitored at 90° to the exciting source, focused through appropriate filters, and isolated by a Jarrell-Ash 3/4 meter Czerney-Turner spectrometer equipped with a cooled (-20°C) EMI 6256S photomultiplier. The three zero-field transitions of DCB were observed at 5.362 GHz, 3.605 GHz and 1.758 GHz, as reported by Buckley and Harris.[12]

In addition to the reported exciton phosphorescence[13] of DCB (origin = 27890 cm^{-1}), emission from a shallow trap which will be referred to as the x trap (origin = 27865 cm^{-1}) and a deep trap which will be referred to as the y trap (origin = 27807 cm^{-1}) was observed. The DCB sample was found to be extremeley sensitive to its recent thermal history. The emission of both the exciton and the x trap was observed at 4.2°K with approximately equal intensity. Upon cooling the sample to 1.3°K only the x trap emission was observed. If the temperature of the DCB crystal was lowered to 4.2°K rapidly (approximately 20 minutes), exciton emission was not observed, but the emission from the y trap was observed in addition to that from the x trap. Upon cooling the sample below 4.2°K, the intensity of the x trap emission increased while the intensity of the y trap emission decreased until at 1.3°K only the x trap emission was observed. The y trap emission is believed to be due to triclinic inclusions in the monoclinic DCB lattice. This was tested by preparing a triclinic sample of DCB which contained approximately 0.01 mole percent p-dimethoxybenzene as an impurity to stabilize the triclinic form at helium temperatures. Since the same phosphorescence origin as well as the same ODMR transition frequencies were observed for both the y trap and the triclinic form of DCB, the y trap is presumably due to triclinic inclusions.

We will concentrate in the remaining discussion on the monoclinic form, i.e., the x trap. Each of the PMDR spectra illustrated in Fig. 1 was obtained while saturating one of the three microwave zero-field transitions. The microwave field was amplitude modulated at 25 cps and the spectra were obtained by standard phase detection techniques. All of the vibronic transitions increase in intensity for each of the PMDR experiments. Since a lock-in amplifier was used, any decrease in intensity while monitoring the emission to a vibrational level of the ground state would have caused the PMDR transition to go negative rather than positive. The relative increase in intensity of the vibronic band at 0,0 + 1579 cm^{-1} (denoted by * in Fig. 1) compared to the origin is striking. The relative increase in intensity of the vibronic band is greatest while saturating the 3.604 GHz transition, while the relative increase in intensity of the origin is greatest for the 5.362 GHz transition. Other vibrations which have been assigned as a_g behave in a manner similar to the origin and therefore it is clear that the vibration at 0,0 +1583 cm^{-1} is not exclusively an a_g vibration as previously assigned, since all vibrations with the same symmetry should maintain a constant intensity ratio within all three PMDR spectra.

C. Adiabatic Inversion

The inversion experiments were conducted at 1.3 ±0.05°K employing essentially the same procedure to be reported elsewhere.[14] Microwave power was obtained from a Hewlett-Packard Model 8690-B sweep oscillator, amplified via a 20 watt traveling wave tube, and was applied to the sample through a rigid coaxial line terminated with a slow wave helix. The frequency sweep required to invert the triplet sublevels was obtained by applying a ramp voltage to the FM input of the microwave sweep generator. The ramp voltage was adjusted so that at V_o the microwave frequency was ω_o, the center of the EPR transition being used for inversion. The FM voltage was swept linearly from $V_o - \frac{1}{2}V$ to $V_o + \frac{1}{2}V$ in a time τ so that the microwave frequency changed from $\omega_o - \frac{1}{2}\delta$ to $\omega_o + \frac{1}{2}\delta$ in a time τ. Maximum inversion was achieved by adjusting the power, the time τ (~100 μsec), and the ramp voltage V. Optimum inversion was obtained at a rate of ~10 MHz/100 μsec.

Simple phosphorescence decay studies at 1.3°K show that the DCB triplet state possesses two short-lived sublevels and one relatively long-lived sublevel. Using the inversion technique the lifetimes of all three sublevels were measured in the same manner as reported by Schmidt, Veeman and van der Waals.[10] The experiment depends upon an examination of the time evolution of the emission intensity to a chosen vibrational band in the phosphorescence spectrum. The event sequence occurred as follows. The excitation source, a 100 joule flash lamp (~20 μsec duration) was triggered first, with the excitation light focused on the sample through a water filter and a Schott 3100 Å interference filter. A PAR waveform eductor was triggered a short time after the excitation flash (~100 μsec) and the population inversion operation[14] was performed after a variable delay which was adjusted to allow the two short-lived spin sublevels to decay. The waveform eductor served to store output from successive event sequences and thereby improve the signal-to-noise ratio. Successive event sequences were separated by a four second delay to insure complete decay of the triplet sublevels. However, only the first one second of each sequence was sampled and stored in the waveform eductor. These observations confirmed the simple decay data, showing the sublevels with 1/e lifetimes of 13 ± 1.5 msec, 46 ± 3 msec, and about 600 msec, and, further, established the long-lived sublevel to be common to both the 5.362 and the 3.604 GHz transitions. Inversion was observed at times as long as several seconds after excitation, thereby establishing that at very low temperatures (~1.3°K) spin-lattice relaxation may be neglected.

Figure 2 illustrates the phosphorescence to the origin in the inversion experiment described above from the accummulation of time average experiments. Following the excitation flash, the two short-lived spin sublevels decay, thus depleting their populations. The inversion operation is triggered after a time long compared to the short lifetimes (~90 msec) thereby placing population from the long-lived sublevel selectively into one of the now almost empty short-lived sublevels. In this manner one can obtain ratios of radiative rate constants from the ratio of intensity of the inversion signal at $\tau = 90$ msec (5.362/3.604 GHz).

From PMDR spectra, vibronic bands of varying symmetries were identified and a systematic series of the 5.362 and 3.604 GHz inversions were also applied to several of the prominent vibrational bands in the phosphorescence spectrum which yielded the data listed in Table I. Monitoring emission from the crystallographic[15] bc face, polarization ratios obtained for this same series of inversions are reported in Table II.

In addition, polarization of emission from the long-lived spin sublevel was measured by eliminating the inversion operation and monitoring the polarized emission in the tail of the phosphorescence decay to vibronic bands at 3629 Å and 3849 Å. Table III illustrates these data.

Discussion

The $T_1 \rightarrow S_o$ phosphorescence, because of its spin-forbidden nature, derives its transition probability from singlet states admixed into the triplet state via spin-orbit coupling.[16] It has been shown that within molecules of relatively high point symmetries the triplet state spin sublevels generally exhibit selective spin-orbit coupling with excited singlet states; consequently, one and sometimes two spin sublevels contribute the majority of phosphorescence intensity.[17]

A completely unambiguous assignment of the orbital symmetry of the triplet states requires, in addition to the polarization of the phosphorescence from the active spin sublevels, a knowledge of the magnetic orientation of these spin sublevels relative to the molecular axes. An explicit consideration of the spin-orbit symmetries for paradichlorobenzene (DCB) in both a $^3B_{1u}$ and a $^3B_{2u}$ state will easily demonstrate this requirement.

Zero-th order wavefunctions for each triplet sublevel, taken as a product of spatial (orbit) and spin functions, transform as the direct product of the irreducible representations of each part. Eigenfunctions of the spin angular momentum operator transform, in zero magnetic field, as rotations which in the point group D_{2h} are $B_{1g}(R_z)$, $B_{2g}(R_y)$, and $B_{3g}(R_x)$. Table IV outlines the total spin-orbit symmetry of the sublevels for the above orbital symmetries for the lowest triplet state of paradichlorobenzene (DCB) in D_{2h}.

An examination of Table IV reveals that the only differences between the $^3B_{1u}$ and the $^3B_{2u}$ assignments are: (1) the spin-orbit symmetry of the τ_x spin sublevel and (2) the magnetic orientation of the B_{3u} and A_u (τ_z or τ_y) spin-orbit states.

We have neglected to consider the two other possible symmetry assignments for the lowest triplet state in DCB (^3A_u) and $^3B_{3u}$), since they correspond to $n\pi^*$ or $\sigma\pi^*$ configurations. Experimental evidence indicates a $\pi\pi^*$ configuration is correct. Early support for this contention came from the observation that the DCB $T_1 \leftarrow S_0$ absorption spectrum exhibits a significant amount of out-of-plane polarization.[6,13] Furthermore, the experimental values for the zero-field parameters D and D* ($D^* = (D^2+3E^2)^{\frac{1}{2}}$) of DCB differ by only a few percent from those of benzene.[12,18] Finally, measurement of the chlorine hyperfine interaction[12] indicates that the para-chlorines of DCB possess a much smaller spin density than might be expected for a $^3n\pi^*$ state.[19]

By analogy to benzene[18,20] and from previous studies of aromatic molecules in $\pi\pi^*$ triplet states,[21 - 29] it is reasonable to assume that in DCB the largest component of the electron spin-spin tensor in its principal axis system is along the molecular axis normal to the plane. In the coordinate system illustrated in Fig. 3, the lowest energy triplet sublevel would then be τ_x.

The observation that the long-lived (~600 msec) spin sublevel is common to both the 3.604 GHz ($D-|E|$) and 5.362 GHz ($D+|E|$) zero-field transitions, together with the above considerations, allows us to assign the lowest energy sublevel as the long-lived sublevel. The remaining spin sublevels, τ_y and τ_z, are then associated with spin eigenfunctions of the zero-field Hamiltonian asymmetry parameter E.

The zero-field splitting parameter E is a measure of the anisotropy of the triplet electron spin distribution in the molecular plane and should be equal to zero if the molecular plane possesses a rotational symmetry greater than C_2. The small but finite value for E measured in benzene[18] requires excess triplet spin density on carbons 2, 3, 5 and 6 (see Fig. 3). It becomes immediately apparent that this spin configuration has the effect of increasing the dipolar repulsion terms along the molecular Z axis. The triplet state sublevels in benzene therefore exist, in order of increasing energy, $\tau_x \ll \tau_y < \tau_z$, corresponding to a positive sign for E. (We have changed the de Groot et al.[18] coordinate system into one similar to the coordinate system used here for DCB to facilitate comparison.)

In the absence of appreciable spin-orbit coupling contributions to the zero-field splittings, the effect on the carbon spin densities with the addition of chlorine substituents to a benzene ring can be understood qualitatively in terms of the one-electron molecular orbitals that form the basis for the excited state. Figure 4 illustrates two possible perturbations that can occur with chlorine para-substitution. Since the chlorine out-of-plane p-orbitals (π) form linear combinations that transform as b_{2g} and b_{3u} in D_{2h} and since the energies of these orbitals would be approximately at the chlorine valence state ionization potential[29] and thus somewhere between the benzene[30] a_{2u} and e_{1g} orbitals, the $b_{2g}(2)$ MO derived from the benzene e_{1g} MO would be raised in energy while the predominantly chlorine $b_{2g}(1)$ MO would be lowered. The b_{3u} interactions unfortunately cannot be easily predicted from first order perturbation theory. Two possible orderings are apparent depending upon the magnitude of the chlorine-benzene interactions. First, the $b_{3u}(3)$ orbital derived from the benzene e_{2u} MO could be lowered via chlorine interactions. This would depend upon many factors, few of which can be even qualitatively estimated. The participation of empty chlorine d-orbitals would, for instance, lower this state relative to its a_u (1) degenerate partner since the a_u state has a node through the para-positions and cannot interact with out-of-plane orbitals. The other possibility is for the $b_{3u}(3)$ MO to increase in energy via carbon-chlorine bonding. The more electronegative the substituent (as would be the case in fluorine substitution) the more likely this situation. In either of the above cases the symmetry of the lowest occupied MO in the ground state of DCB is expected to be $b_{2g}(2)$; therefore two excited state orbital symmetries can arise. B_{1u} is derived from a $b_{2g} \rightarrow b_{3u}$ transition while the state B_{2u} is derived from the transition $b_{2g} \rightarrow a_u$. If we consider the triplet states with one of the unpaired electrons in the $b_{2g}(2)$ MO and the other in an a_u (1) or $b_{3u}(3)$ MO, the sign of the spin dipolar term E can be anticipated in each case knowing that the para-substitution does not appreciably affect the value of D. Aside from a small delocalization of the electron spin on the two chlorines the distribution of the spin density on the carbons of the ring is given by the carbon coefficients in each one-electron MO. Since both the $a_u(1)$ and $b_{1g}(3)$ MO's (Cf. Figure 5) have a nodal plane through the 1 and 4 positions the spin density in these MO's would be concentrated on positions 2, 3, 5 and 6. Carbon 2, 3, 5 and 6 coefficients in the b_{2g} and b_{3u} MO's are only about half those of carbon 1 and 4; consequently the para-carbons have four times the spin density of the others in these MO. Naturally the chlorine affects these coefficients to a degree by delocalizing a small amount of spin density as evidenced by the out-of-plane chlorine hyperfine coupling constant (~25 MHz).[12] Figure 5 summarizes the spin densities on each carbon and the symmetries for the appropriate one-electron MO's. Table V summarizes the appropriate spin sublevel ordering and spin densities for the two possible orbital symmetries $^3B_{1u}$ and $^3B_{2u}$ in para-dichlorobenzene and s-tetrachlorobenzene (TCB). It is expected that the lowest occupied MO in TCB would be $b_{1g}(1)$; however the ambiguity of the first unoccupied MO remains the same as in DCB. In the case of TCB, chlorine d-orbitals would tend to lower the a_u relative to the $b_{3u}(3)$ MO. In either molecule in both the $^3B_{1u}$ and $^3B_{2u}$ excited states the direction and a rough estimate of the in-plane spin dipolar repulsion can be ascertained using the spin densities in Table V. Consider, for example, the $^3B_{1u}$ state in DCB. The spin density is principally localized on the para-carbon positions; thus the dipolar repulsion between carbons 2-3 and 5-6 is reduced resulting in the τ_z spin sublevel being lower in energy than τ_y. In addition the E values should be "large". On the other hand, a DCB $^3B_{2u}$ state would show a "small" E value since the spin density is uniformly distributed over the carbons except for the fact that the para-carbon spin density would be less than the remaining carbons because of the spin delocalization on the chlorines; thus the largest dipolar interactions would be along z. Consequently τ_z would be higher in energy than τ_y. These arguments have been extended to TCB (cf. Table V). It is noteworthy that in either symmetry $^3B_{1u}$ or $^3B_{2u}$ the spin-orbit symmetry associated with the highest spin sublevel is B_{3u} in DCB and A_u in TCB. This is consistent with the observation that phosphorescence to the origin in DCB (see below) and in TCB[31] originates from the upper (B_{3u}) and middle (B_{3u}) spin sublevels, respectively, in DCB and TCB.

One can argue for a $^3B_{1u}$ assignment in both molecules based upon the fact that the measured E values in both molecules are rather large. In fact, in DCB[12] it is 65% of its maximum allowed value and in TCB[32] it is 70% of its maximum allowed value before the principal coordinate system of the zero-field Hamiltonian must be changed.[9] This we believe is a large enough anisotropy in the zero-field splitting to provide evidence for a $^3B_{1u}$ assignment for both DCB and TCB.

The application of an external magnetic field could in principle verify the sublevel order. Such a field application has been attempted on DCB in this laboratory, but the unfavorable orientation of the two molecules in the DCB unit cell[15] prevented us from obtaining conclusive data by a low magnetic field ODMR study.

The ordering of the spin-orbit states in DCB has been established by determining which spin sublevel has the largest radiative dipole activity to the phosphorescence origin. Since in D_{2h} the spin sublevel that transforms as A_u is formally dipole forbidden, the principal activity should be from the spin sublevel that transforms as B_{3u}. In the $^3B_{1u}$ or $^3B_{2u}$ states this would correspond to τ_y or τ_z respectively. Delayed adiabatic inversion data illustrated in Fig. 2 and Table I demonstrate that the principal activity is from the upper spin sublevel. The important point of Fig. 2 is that the ratio of the radiative rates (τ_y/τ_z) is much greater than unity. Accepting the qualitative description of E above as correct, these data tentatively establish the symmetry of the phosphorescent triplet in DCB as $^3B_{1u}$.

The $^3B_{1u}$ assignment is further substantiated by polarization measurements (cf. Table III) taken while monitoring emission from the DCB crystallographic bc face[15] in the tail of the phosphorescence decay to vibrational bands at 3529 Å (0,0 + 309 cm^{-1}) and 3849 Å (0,0 + (1579+309) cm^{-1}) which have been assigned as a b_{2g} fundamental[6,33] and a $b_{1g}(b_{3g} \times b_{2g})$ combination band[34] respectively. These measurements indicate that emission from the long-lived sublevel (τ_x) is out-of-plane polarized to the b_{1g} band, while polarization is mixed to the b_{2g} band. In addition, phosphorescence from τ_x to the b_{1g} band is about two and one-half times as intense as that to the b_{2g} when the emission is normalized to their respective total phosphorescence intensity. These data point to a B_{2u} spin-orbit symmetry for the τ_x sublevel consistent with the $^3B_{1u}$ orbital assignment (cf. Table IV).

It is apparent from the data that the B_{3u} and A_u spin-orbit states contribute most to the dipole activity in DCB phosphorescence. This activity and our observation that the lowest triplet state of DCB possesses two short-lived (lifetimes: 13 ± 1.5 msec and 46 ± 3 msec) and one relatively long-lived spin sublevel (~600 msec) can be understood when further aspects of the chlorine perturbations are considered more explicitly.

Intrinsic emission lifetimes of the triplet sublevels are inversely proportional to the radiative and/or radiationless transition probability, and thereby proportional to the amount of singlet character mixed into the triplet state primarily by spin-orbit coupling. The measured magnitudes of the DCB triplet sublevel lifetimes (τ_y and τ_z) are about a factor of 10^3 shorter than those of benzene.[35] This observation points to a significant amount of spin-orbit coupling presumably due to the addition of two chlorine nuclei to the benzene ring. A natural assumption then is that the most effectively spin-orbit coupled singlet states would be those states formed from molecular orbitals which include to a large degree the atomic orbitals of the two para-chlorines. The symmetries of these possible chlorine perturbing orbitals using all chlorine valence electrons except the out-of-plane p_π are b_{1u}, a_g, b_{2u}, b_{3g}.

The lowest unoccupied molecular orbital in benzene has e_{2u} symmetry.[30] In the point group D_{2h} the e_{2u} MO reduces to a b_{3u} and an a_u MO. Singlet states fashioned from the combinations of these molecular orbitals and the molecular orbitals admixed with para-chlorine atomic orbitals will transform as the direct products of their respective irreducible representations. Singlet states which might admix any electric dipole character into the triplet sublevels must be antisymmetric with respect to inversion. This restriction limits the consideration of possible perturbing singlet states to $^1B_{3u}$ ($b_{3g} \times a_u$(B); $a_g \times b_{3u}$(B)) and ^1A_u ($a_g \times a_u$(B); $b_{3g} \times b_{3u}$(B)) (where B denotes MO derived from benzene e_{2u} in D_{2h} symmetry). Also, the presence of carbon-chlorine bonds (as opposed to carbon-hydrogen bonds) would lower the energy of some $\sigma\pi^*$ states of A_u and B_{3u} symmetry relative to those in benzene. Finally, the A_u and B_{3u} states have one-center spin-orbit coupling matrix elements with the τ_z and τ_y sublevels while the $^1\pi\pi^*$ character associated with τ_x arises only from two-center spin-orbit terms.[17] Consequently one might expect most of the phosphorescence to originate from τ_y and τ_z as the experimental data demonstrate.

We have excluded from discussion vibronic coupling in the singlet and triplet manifolds. This topic deserves special attention and is the subject of another investigation.[31]

While the ODMR techniques employed in this study have helped remove the primary ambiguities (i.e., spin sublevel origins of phosphorescence), the present observations of DCB phosphorescence are subject to other ambiguities which also plagued previous investigators, i.e., crystal field effects and possible changes in the excited state geometry. In fact, both the polarized and nonpolarized inversion data (Tables I and II) point to a significant relaxation of D_{2h} symmetry restrictions in the phosphorescence emission.

The D_{2h} symmetry restrictions require that emission to any totally symmetric vibration should originate from the $\tau_y(B_{3u})$ sublevel, while the $\tau_z(A_u)$ sublevel should be completely inactive to such vibrations. The measured value of the radiative rate constant ratio for $\tau_y(B_{3u}):\tau_z(A_u)$ to the origin (Table I) is only about 4:1. Moreover, while emission from τ_y shows predominantly out-of-plane polarization as expected, emission from τ_z displays a slight in-plane polarization. Further, it is found that the primary emission route to <u>every</u> vibrational band in the phosphorescence spectrum is from the $\tau_y(B_{3u})$ sublevel, and that every band also derives a significant amount of intensity from the $\tau_z(A_u)$ sublevel. This can be seen from the ratios reported in Table I which are approximately equal to the spin sublevel radiative rate constant ratios for the vibrational bands listed.

The PMDR spectra shown in Fig. 1 clearly reveal that all optical transitions are coupled by all three microwave transitions.

The vibrational band found at 3804 Å (0,0 + 1579 cm^{-1}) is most perplexing in this respect. This band has been assigned as an a_g fundamental by some investigators.[6,36,37] PMDR spectra (Fig. 1) clearly show that it behaves differently than other a_g vibrations. A tentative b_{3g} assignment was therefore made on the basis of reported laser Raman studies;[33] however, the microwave inversion data subsequently failed to display the expected b_{3g} behavior for this band. Any b_{3g} band in the phosphorescence spectrum would be expected to exhibit a reversal of activity from spin sublevels τ_y and τ_z compared to the origin (or any totally symmetric vibration). Even taking into account a slight relaxation of symmetry restriction we would expect most of its intensity to be derived from the $\tau_z(A_u \times b_{3g} = B_{3u})$ sublevel. Our observations, in fact, show a marked increase in emission from the τ_z sublevel in the PMDR's. However, most of the emission remains from τ_y, as evident from the radiative rate constant ratios from τ_y and τ_z, i.e., $k_{r\tau_y}^{(0,0+1579)} : k_{r\tau_z}^{(0,0+1579)} =$ 1.4 : 1. These anomalous characteristics allow us to suggest that the (0,0 + 1579 cm^{-1}) band is, in actuality, associated with both an a_g and a b_{3g} vibration which our instruments were unable to resolve.

A definitive explanation for the mixed phosphorescence observed in DCB is beyond the scope of data currently available. We have, however, considered various possibilities. Explicit considerations of the crystal field effects focused on the surrounding chlorine atoms, since the reduction of molecular symmetry D_{2h} to C_i site symmetry would occur in all likelihood via the chlorine crystal field contributions (e.g., the heavy atom effect). An analysis of the DCB crystal structure[15] shows that the sum of weighted ($1/|r|^2$) vectors from each of the 24 nearest chlorine atoms surrounding any DCB molecule yields a resultant vector $0.87\ \hat{x} + 0.31\ \hat{y} + 0.38\ \hat{z}$, relative to the DCB molecular axes. Such a field vector could mix both the in-plane zero-field spin sublevels and the out-of-plane spin sublevel with each in-plane spin state. Obviously, this chlorine-field vector possesses suitable geometry to account for the mixed DCB phosphorescence, but a quantitative assessment of the strength of the external chlorine influence will be necessary before we can venture any definite conclusions.

Aside from crystal-field effects, the relaxation of symmetry restrictions observed in DCB trap phosphorescence might also be due to a distortion of the molecule itself. However, the question of the exact nature of this distortion remains as yet unanswered. The distortion may be caused by a rearrangement of the nuclear skeleton either under the influence of the excited state electronic potential or as an inherent characteristic of the trap. It is noteworthy, however, that the chlorine field gradient in the excited state is substantially lower than in the ground state. As has been discussed[12] this can be due in part to a distortion and in part to increased carbon-chlorine π bonding in the excited state. The average decrease in chlorine field gradients in $\pi\pi^*$ states in those molecules thus far investigated where no distortion is suspected is about 3% (8-chloroquinoline,[38] 1,2,4,5-tetrachlorobenzene,[31] and 1,4-dichloroquinoxaline[39]). An average decrease of 3% may well represent the increased π character of the C-Cl bond. DCB, on the other hand, shows an 8% decrease in the chlorine field gradient. Perhaps the additional

5% decrease is due to an out-of-plane chlorine distortion. The PMDR and inversion data do not exclude this possibility. Further experiments are needed to resolve this question adequately.

Attempts made in this laboratory to observe the ODMR spectra of DCB doped into suitable hosts (known crystal structure and an absence of heavy atoms) have as yet proved unsuccessful.

Acknowledgements

This work was performed with the support of the Inorganic Materials Research Division of the Lawrence Berkeley Laboratory under the auspices of the U. S. Atomic Energy Commission. We are grateful and appreciative of fruitful discussions with Professor A. H. Maki, University of California, Riverside, and Dr. J. E. Williams, Jr., and J. Cambray at the University of California, Berkeley.

References

1. H. Shull, J. Chem. Phys. 17, 295 (1949).
2. D. S. McClure, J. Chem. Phys. 17, 665 (1959); D. P. Craig, J. Chem. Phys. 18, 236 (1950).
3. M. Goeppert-Mayer and A. L. Sklar, J. Chem. Phys. 6, 645 (1938); C. C. J. Roothaan and R. S. Mulliken, J. Chem. Phys. 16, 118 (1948); C. C. J. Roothaan and R. G. Parr, J. Chem. Phys. 17, 1001 (1949); R. G. Parr, D. P. Craig, and I. G. Ross, J. Chem. Phys. 18, 1561 (1950); K. J. Niira, J. Chem. Phys., 20, 1498 (1952); J. Phys. Soc. Japan, 8, 630 (1953); J. A. Pople, Proc. Phys. Soc. (London) A68, 81 (1955); R. Pariser, J. Chem. Phys. 24, 250 (1956); N. S. Ham and K. Ruedenberg, J. Chem. Phys. 25, 1 (1956); D. R. Kearns, J. Chem. Phys. 36, 1608 (1962); J. R. Platt, J. Mol. Spectroscopy 9, 288 (1962); J. W. Moskowitz and M. P. Barnett, J. Chem. Phys. 39, 1557 (1963); J. M. Schulman and J. W. Moscowitz, J. Chem. Phys. 43, 3287 (1965).
4. A. C. Albrecht, J. Chem. Phys. 33, 156 (1960); 33, 169 (1960); 38, 354 (1962).
5. D. W. Olds, J. Chem. Phys. 35, 2248 (1961).
6. G. Castro and R. M. Hochstrasser, J. Chem. Phys. 46, 3617 (1967).
7. R. M. Hochstrasser and T.-S. Lin, J. Chem. Phys. 49, 4929 (1968).
8. M. Sharnoff, J. Chem. Phys. 46, 3263 (1967); A. L. Kwiram, Chem. Phys. Letters 1, 272 (1967); J. Schmidt, I. A. M. Hesselmann, M. S. de Groot and J. H. van der Waals, Chem. Phys. Letters 1, 434 (1967); J. Schmidt and J. H. van der Waals, Chem. Phys. Letters 2, 640 (1968); 3, 546 (1969); I. Y. Chan, J. Schmidt and J. H. van der

Waals, Chem. Phys. Letters 4, 269 (1969); C. B. Harris, D. S. Tinti, M. A. El-Sayed and A. H. Maki, Chem. Phys. Letters 4, 409 (1969); M. J. Buckley, C. B. Harris and A. H. Maki, Chem. Phys. Letters 4, 591 (1970); M. A. El-Sayed, D. S. Tinti and D. Owens, Chem. Phys. Letters 3, 339 (1969); M. A. El-Sayed, J. Chem. Phys. 52, 6432 (1970); D. S. Tinti and M.A. El-Sayed, J. Chem. Phys. 54, 2529 (1971); M. A. El-Sayed, J. Chem. Phys. 52, 6432 (1970); M. D. Fayer, C. B. Harris and D. A. Yuen, J. Chem. Phys. 53, 4719 (1970); C. B. Harris, J. Chem. Phys. 54, 972 (1971); A. H. Francis and C. B. Harris, Chem. Phys. Letters 9, 181 (1971); J. Schmidt, V. C. van Dorp and J. H. van der Waals, Chem. Phys. Letters 8, 345 (1971); M. Sharnoff, Chem. Phys. Letters 2, 498 (1968); R. F. Clements and M. Sharnoff, Chem. Phys. Letters 7, 4 (1970).

9. A. Carrington and A. D. McLachlan, *Introduction to Magnetic Resonance* (Harper and Row, New York, 1967), pp. 115-127.
10. J. Schmidt, W. S. Veeman and J. H. van der Waals, Chem. Phys. Letters 4, 341 (1969).
11. D. S. Tinti, M. A. El-Sayed, A. H. Maki and C. B. Harris, Chem. Phys. Letters 3, 343 (1969).
12. M. J. Buckley and C. B. Harris, J. Chem. Phys. 56, xxx (1972).
13. G. A. George and G. C. Morris, Mol. Cryst. and Liq. Cryst. 11, 61 (1970).
14. C. B. Harris and R. J. Hoover, J. Chem. Phys., in press.
15. U. Croatto, S. Bezzi and E. Bua, Acta Crystl. 5, 825 (1952).
16. D. S. McClure, J. Chem. Phys. 20, 682 (1952).
17. S. P. McGlynn, T. Azumi and M. Kinoshita, *Molecular Spectroscopy of the Triplet State* (Prentice-Hall, Englewood Cliffs, N.J., 1969).

18. M. S. de Groot, I. A. M. Hesselmann and J. H. van der Waals, Mol. Phys. 16, 45 (1969).

19. L. T. Cheng and A. L. Kwiram, Chem. Phys. Letters 4, 457 (1969).

20. M. Godfrey, C. W. Kern and M. Karplus, J. Chem. Phys. 44, 4459 (1966).

21. M. Gouterman and W. Moffitt, J. Chem. Phys. 30, 1107 (1959).

22. M. Gouterman, J. Chem. Phys. 30, 1369 (1959).

23. B. Smaller, J. Chem. Phys. 37, 1579 (1962).

24. H. Hameka, J. Chem. Phys. 31, 315 (1959).

25. Y. N. Chin, J. Chem. Phys. 39, 2736 (1963).

26. C. A. Hutchison, Jr. and B. W. Magnum, J. Chem. Phys. 34, 908 (1961).

27. N. Hirota, C. A. Hutchison, Jr., and P. Palmer, J. Chem. Phys. 40, 3717 (1964).

28. C. A. Hutchison, Jr., J. V. Nicholas and G. W. Scott, J. Chem. Phys. 53, 1906 (1970).

29. C. E. Moore, "Atomic Energy Levels", U.S. National Bureau of Standards, Circular 467, U. S. Printing Office, Washington, D.C., 1949 and 1952.

30. L. Salem, The Molecular Orbital Theory of Conjugated Systems (W. A. Benjamin, New York, 1966).

31. A. H. Francis and C. B. Harris, unpublished work.

32. A. H. Francis and C. B. Harris, Chem. Phys. Letters 9, 188 (1971).

33. M. Suzuki and M. Ito, Spectrochim. Acta 25A, 1017 (1969).

34. See later text for discussion of this band. We suggest that this band is actually a $b_{1g}(b_{3g} \times b_{2g})$ combination band coincident with a $b_{2g}(a_g \times b_{2g})$ combination band.

35. D. S. McClure, J. Chem. Phys. 17, 905 (1949).

36. A. Stojiljkovic and D. H. Whiffen, Spectrochim. Acta 12, 47 (1958).

37. J. R. Scherer and J. C. Evans, Spectrochim. Acta 19, 1739 (1963).

38. M. J. Buckley and C. B. Harris, Chem. Phys. Letters 5, 205 (1970).

39. M. J. Buckley and C. B. Harris, unpublished work.

40. Note added in preparation: Similar techniques have recently been applied to determine the orbital symmetry of the lowest excited triplet state in benzene. The reader is referred to A. A. Gwaiz, M. A. El-Sayed and D. S. Tinti, Chem. Phys. Letters 9, 454 (1971).

TABLE I

Relative Inversion Heights
(Normalized to phosphorescence intensity)

	$D+\|E\|$	$D-\|E\|$	Ratio $\frac{D+\|E\|}{D-\|E\|}$[b]
Origin (0,0)	0.50	0.12	4.1 : 1
$b_{1g}(0,0 +(1579+309)\ cm^{-1})$[a]	0.47	0.18	2.6 : 1
$b_{2g}(0,0 + 309\ cm^{-1})$	0.53	0.12	4.6 : 1
$b_{3g}(0,0 + 1579\ cm^{-1})$[a]	0.40	0.28	1.4 : 1

[a] See text for discussion of assignments of these bands.

[b] These ratios are approximately equal to the radiative rate constant ratios (τ_y/τ_z) in the bands listed.

TABLE II

Polarized Inversion Heights (b/c ratio)

	D+|E|	D-|E|
Origin (0,0)	0.49	1.45
$b_{1g}(0,0 + (1579+309)\ cm^{-1})$	0.95	1.38
$b_{2g}(0,0 + 309\ cm^{-1})$	0.83	1.67
$b_{3g}(0,0 + 1579\ cm^{-1})$	0.65	1.00

TABLE III

b/c polarization ratios in the phosphorescence decay*

	Origin	b_{1g}	b_{2g}	b_{3g}
τ_y, τ_z (0-25 msec)	0.7	1.4	1.4	0.7
τ_x (200 msec - 1 sec)	0.5	0.8	1.1	0.6

* The a'c face shows similar a'/c ratios.

TABLE IV

The spin-orbit symmetries of the individual magnetic sublevels in paradichlorobenzene in the states $^3B_{1u}$ and $^3B_{2u}$

Orbital Symmetry	Magnetic Sublevel	Spin-orbit Symmetry	Vibrational Band Polarization[a]			
			a_g	b_{1g}	b_{2g}	b_{3g}
$^3B_{1u}(\pi\pi^*)$	τ_y	B_{3u} $(n\pi^*)$	X	Y	Z	-
	τ_z	A_u $(n\pi^*)$	-	Z	Y	X
	τ_x	B_{2u} $(\pi\pi^*)$	Y	X	-	Z
$^3B_{2u}(\pi\pi^*)$	τ_z	B_{3u} $(n\pi^*)$	X	Y	Z	-
	τ_y	A_u $(n\pi^*)$	-	Z	Y	X
	τ_x	B_{1u} $(\pi\pi^*)$	Z	-	X	Y

[a] Z and Y are in-plane long and short axes, respectively, according to the coordinate system in Fig. 3, while X is out-of-plane.

TABLE V

Molecule	Triplet State	Predicted Spin Sublevel Order (Spin-Orbit Symmetry)	E Value	Approximate Carbon Spin Densities					
				1	2	3	4	5	6
DCB	$^3B_{1u}$ $(b_{2g} \rightarrow b_{3u})$	$\tau_y > \tau_z \gg \tau_x$ $(B_{3u} > A_u \gg B_{2u})$	"large" negative	0.67*	0.165	0.165	0.67*	0.165	0.165
DCB	$^3B_{2u}$ $(b_{2g} \rightarrow a_u)$	$\tau_z > \tau_y \gg \tau_x$ $(B_{3u} > A_u \gg B_{1u})$	"small" positive	0.33*	0.33	0.33	0.33*	0.33	0.33
TCB	$^3B_{1u}$ $(b_{1g} \rightarrow a_u)$	$\tau_z > \tau_y \gg \tau_x$ $(A_u > B_{3u} \gg B_{2u})$	"large" positive	~0	0.5*	0.5*	~0	0.5*	0.5*
TCB	$^3B_{2u}$ $(b_{1g} \rightarrow b_{3u})$	$\tau_y > \tau_z \gg \tau_x$ $(A_u > B_{3u} \gg B_{1u})$	"small" negative	0.33	0.33*	0.33*	0.33	0.33*	0.33*

* Indicates appropriate chlorine positions. At these positions spin density values are a maximum since any spin delocalization on chlorines bonded to these carbons would reduce the carbon spin densities.

Figure Captions

Figure 1. (a) Unpolarized phosphorescence spectrum in para-dichlorobenzene.

(b) The 5.362 GHz (D+|E|) zero-field PMDR spectrum.

(c) The 3.604 GHz (D-|E|) zero-field PMDR spectrum.

(d) The 1.758 GHz (2|E|) zero-field PMDR spectrum.

All spectra were obtained at 1.3°K.

Figure 2. The phosphorescence decay and microwave induced inversion monitoring the x-trap origin at 1.3°K in para-dichlorobenzene from 168 accumulations in a 100 channel averager. The fraction of inversion in both transitions was 0.85.

Figure 3. Para-dichlorobenzene zero-field splittings for the phosphorescent triplet state in the coordinate system illustrated.

Figure 4. The one-electron π molecular orbitals of benzene and para-dichlorobenzene with a qualitative assessment of two possible effects of the para-chlorine substitution.

Figure 5. The symmetries of various benzene one-electron molecular orbitals in D_{2h} along with approximate spin density distributions on the individual carbon atoms in the appropriate molecular orbitals.

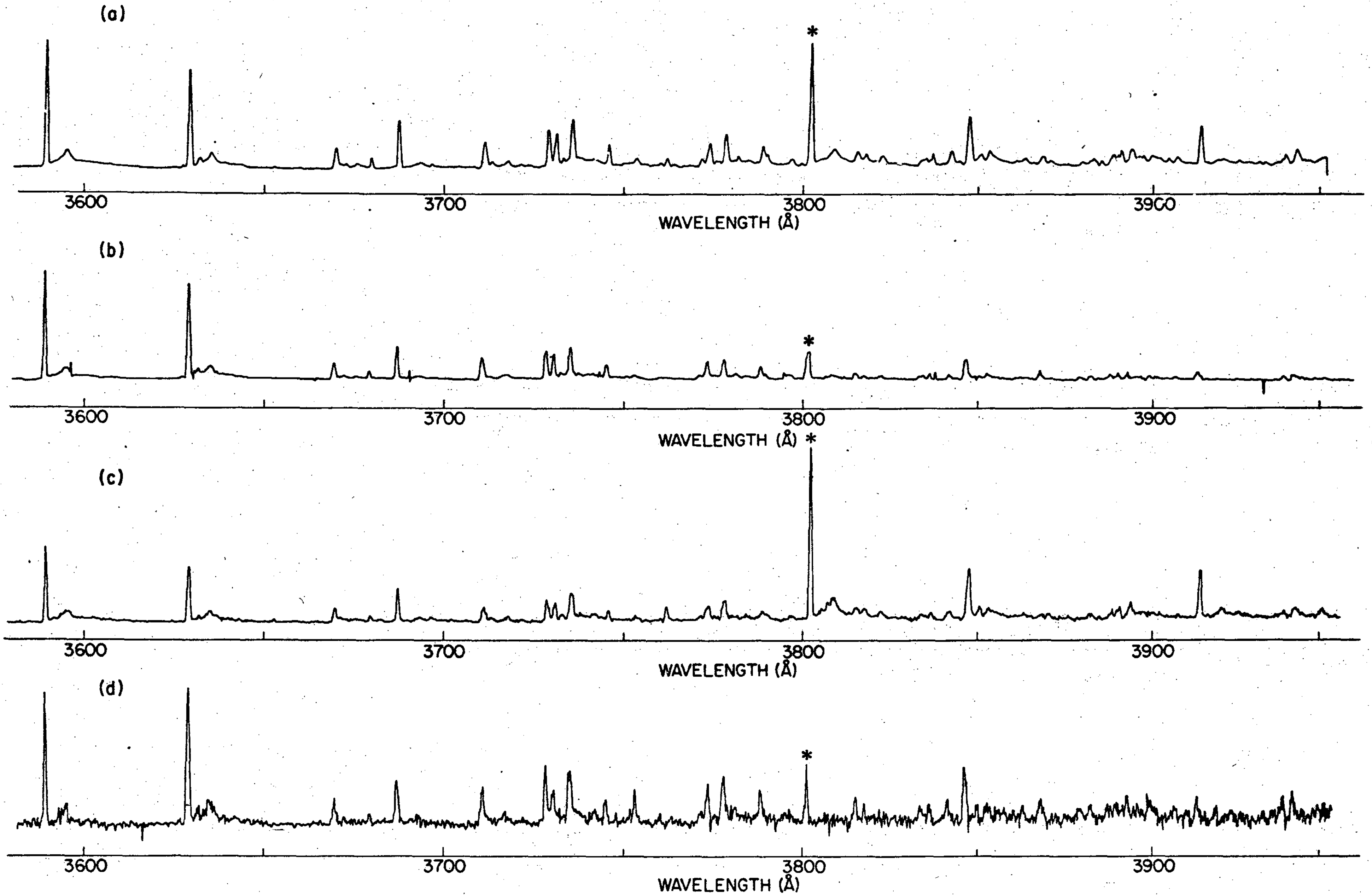

XBL 7111-7520

Fig. 1

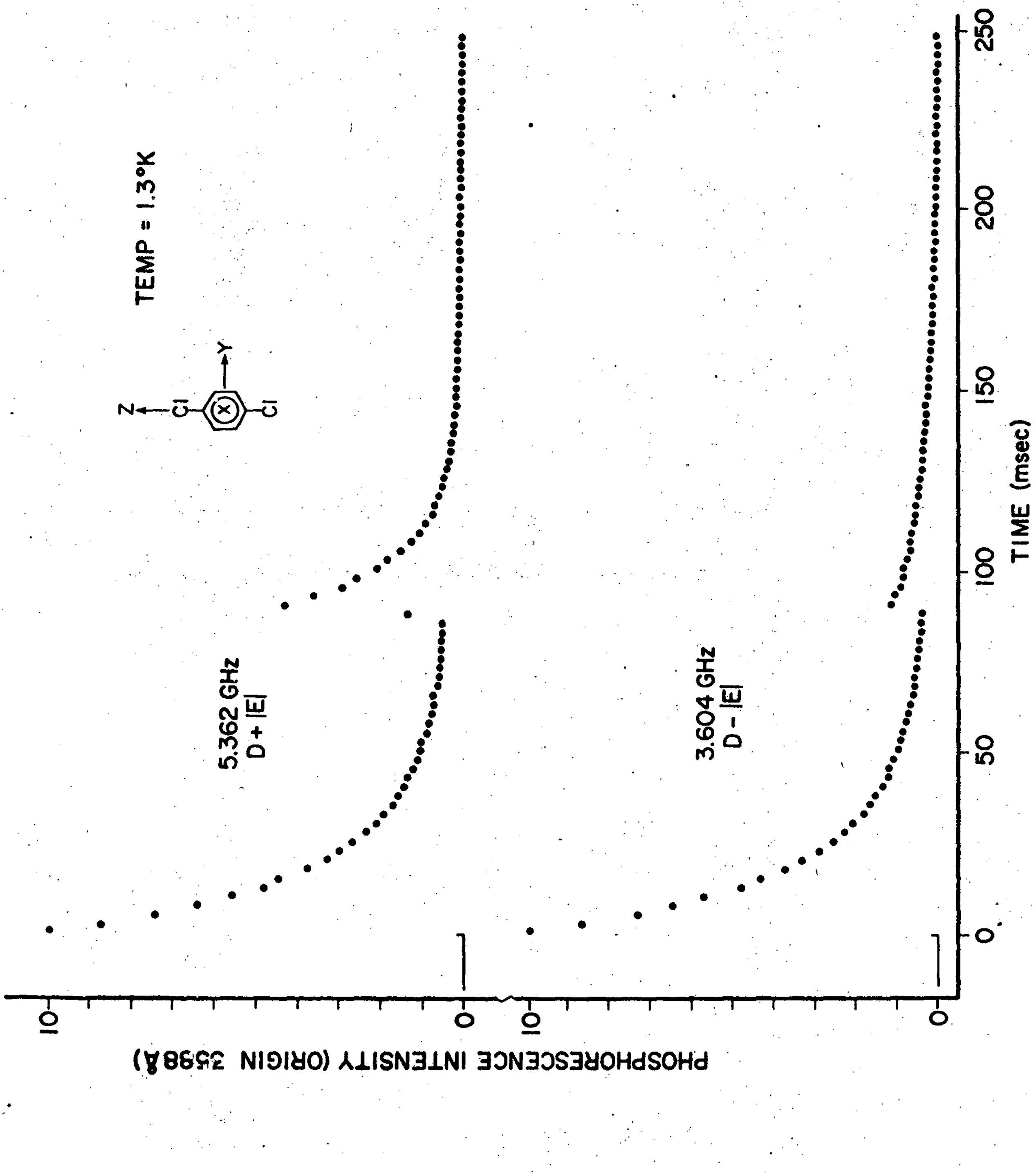

XBL 717-6924

Fig. 2

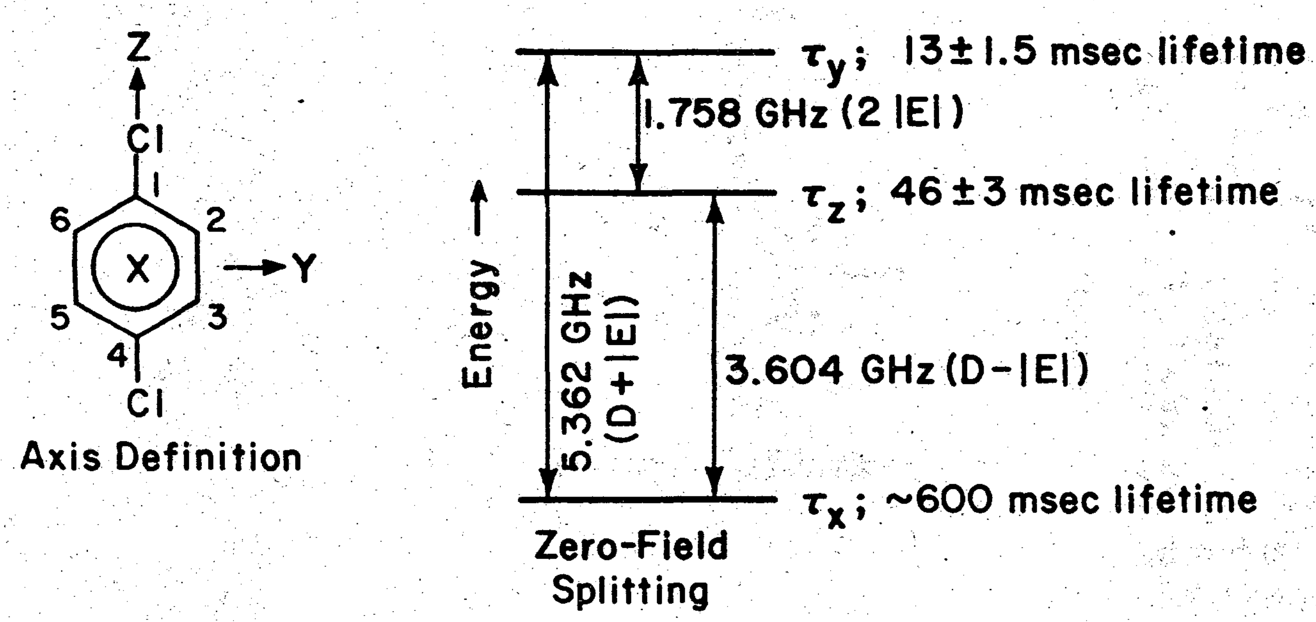

XBL 7111-7522

Fig. 3

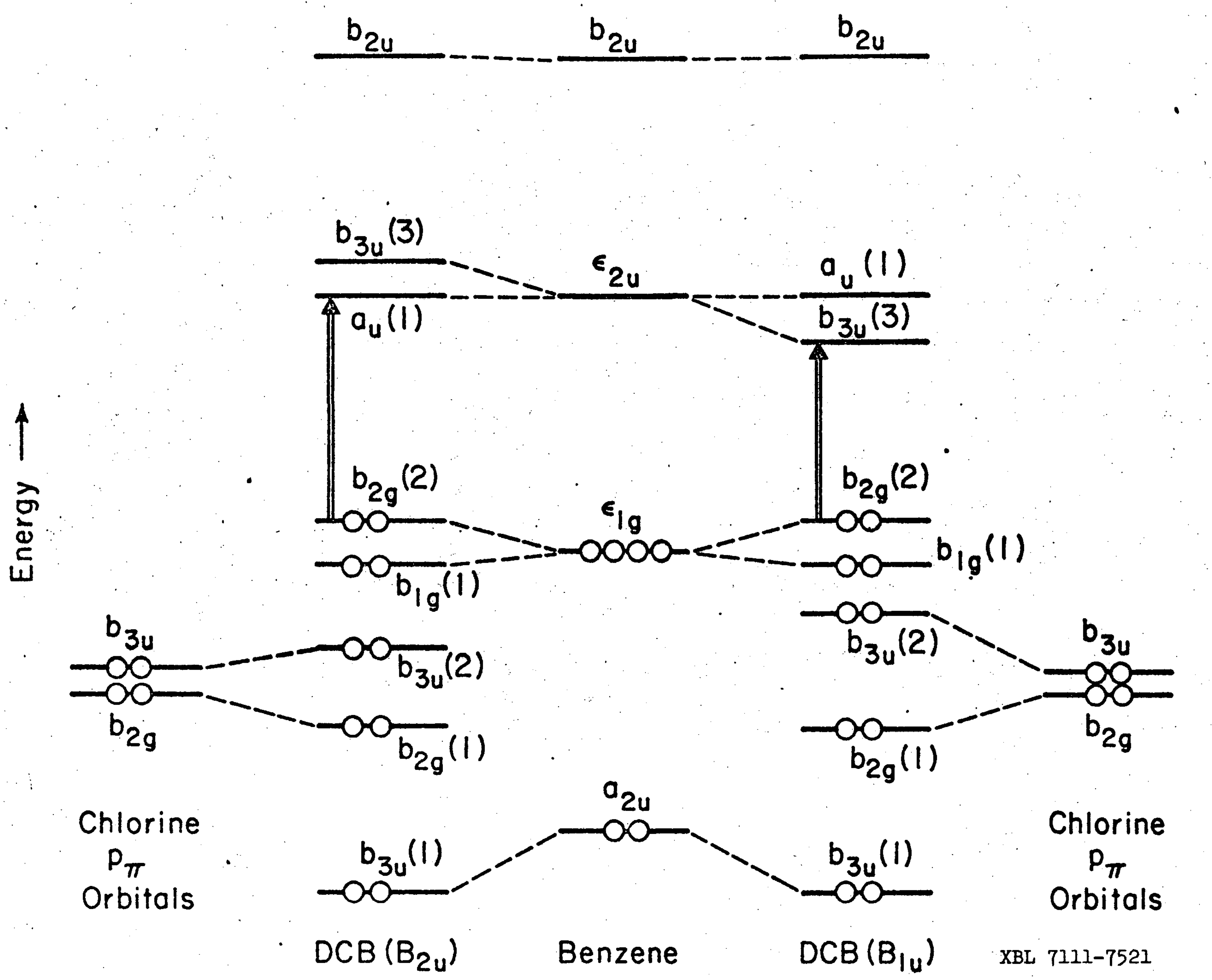

Qualitative Effects of Parachlorine Substitution in the Benzene π-Orbitals.

XBL 7111-7521

Fig. 4

Symmetry and Spin Density Distribution in Substituted Benzene One-Electron Molecular Orbitals.

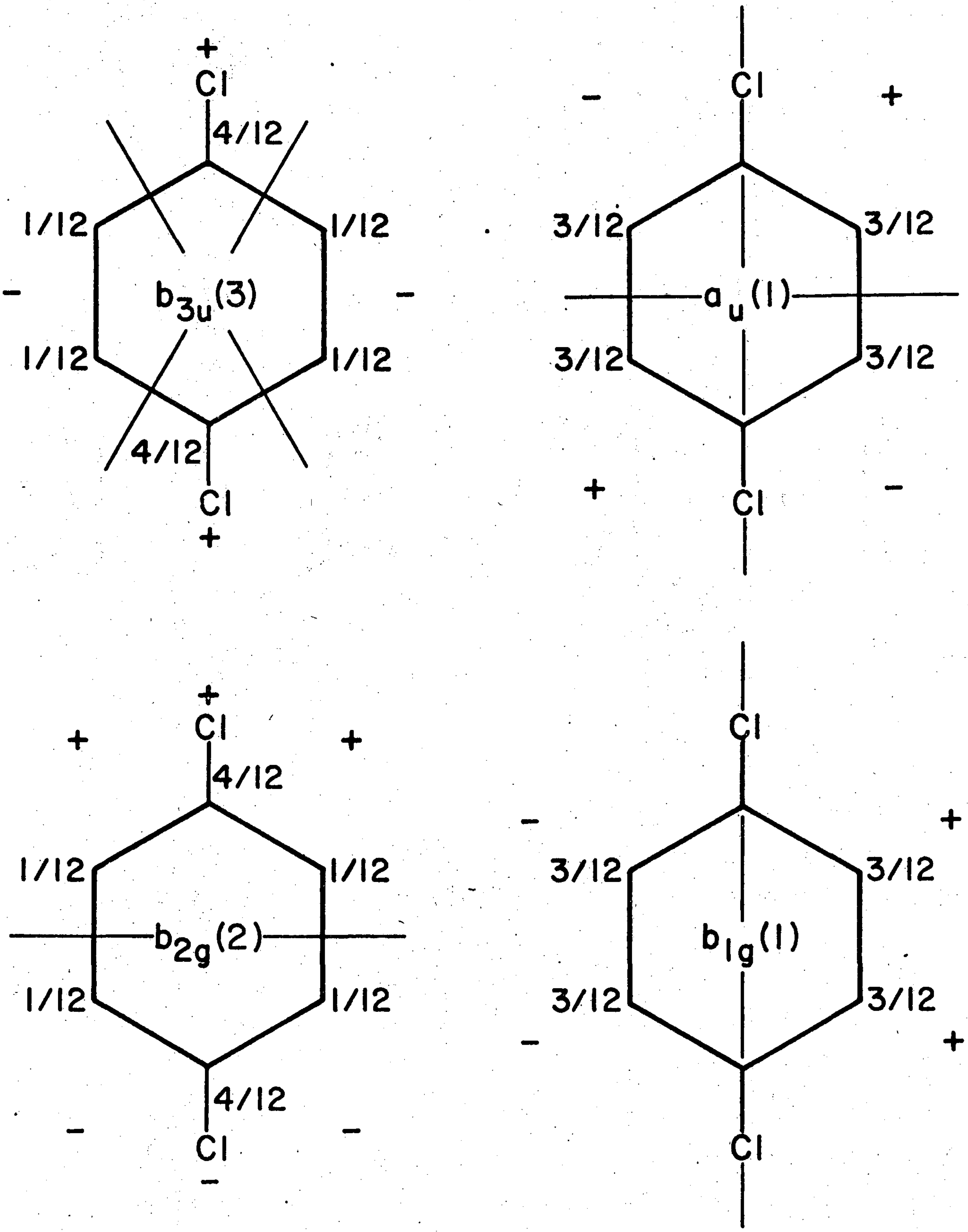

Fig. 5

XBL 7111-7523

TECHNICAL INFORMATION DIVISION
LAWRENCE BERKELEY LABORATORY
UNIVERSITY OF CALIFORNIA
BERKELEY, CALIFORNIA 94720